Fast and Accurate Analysis of Waveguide Filters by the Coupled-Integral-Equations Technique

Smain Amari, Jens Bornemann, *Senior Member, IEEE,* and Rüdiger Vahldieck, *Senior Member, IEEE*

Abstract— The coupled-integral-equations technique (CIET) is successfully applied to accurately determine the frequency response of waveguide filters in a *single step*. A four-resonator H-plane filter is analyzed by the mode-matching technique (MMT) and the CIET for comparison and results in a reduction of central-processing-unit (CPU) time of the order of 400. A set of CIE's for the tangential electric fields at the apertures of the discontinuities are derived and solved by the moment method. Basis functions, which include the edge conditions at each of the discontinuities, are used to achieve numerical efficiency. It is shown that 1–4 basis functions, which include the edge conditions, are sufficient over a broad range of frequencies. The inclusion of the edge conditions in the basis functions is shown to have a dramatic effect on the convergence of the CIET, especially for narrow-band filters.

Index Terms— Computer-aided design, integral equations, mode-matching methods, moment methods, waveguide filters.

I. INTRODUCTION

MICROWAVE filters are widely used components in modern microwave communications systems. Waveguide technology is often employed in implementing these frequency selective devices whose frequency response must be accurately predicted before the actual implementation is carried out in order to save cost and time.

The mode-matching technique (MMT) is a popular approach in the design and analysis of modern waveguide filters [1]. In this technique, the generalized scattering matrices of the individual discontinuities are cascaded to determine the overall frequency response of the filter. From a computational point of the view, the problem is then reduced to accurately determine the generalized scattering matrices of each discontinuity.

However, the method is known to exhibit the phenomenon of relative convergence which is often overcome by a judicious choice of the number of modes retained in the modal expansions on each side of the discontinuity [2]. When two discontinuities are strongly interacting it becomes necessary to include a large number of modes which results in large generalized scattering matrices.

An examination of the underlying principles of the MMT shows that the modes of the sections of the waveguides are given an unduly important role. It is certainly true that the dominant physics of the problem takes place at the discon-

tinuities and not in the uniform sections of the waveguides. Unfortunately, the normal modes contain information about the uniform sections, through the boundary conditions, but not about the discontinuities. Therefore, we propose to modify the MMT in such a way that the problem is reformulated in terms of the fields at the discontinuities through an appropriate choice of basis functions and in an integral form. By directly concentrating on the field at the discontinuity, which is described by a single function for both of the uniform sections of the waveguides, the phenomenon of relative convergence is eliminated as the modes of the two sides are given only a minor role.

In addition, when two adjacent discontinuities are strongly interacting, their field distributions only slightly differ. It is no longer necessary to use a large number of basis functions to describe the overall frequency response of the two discontinuities. A *fortiori*, it is possible to reformulate the entire scattering problem of the filter in one step, in terms of the fields at each of the discontinuities. By doing so, the edge conditions at each of the discontinuities are all included and the interaction between all the discontinuities are accurately described regardless of the strength of their interactions. The resulting formulation is a set of CIE's for the tangential electric fields at the different discontinuities. Mathematically, the present formulation leads to a Riemann–Hilbert problem (RHP) of systems of singular integral equations [3]. The technique has been recently applied to the case of up to three septa in a rectangular waveguide as well as to rectangular ridge waveguides [4], [5].

In this paper, we apply the coupled-integral-equations technique (CIET) to the analysis of H-plane waveguide filters. Numerical results obtained from the CIET are compared to those from the MMT to demonstrate the accuracy and speed of the technique. The paper is organized as follows. Section II describes the CIET as it applies to H-plane filters along with the basis functions which include the edge conditions. Typical numerical results from the CIET and the MMT for two four-resonator designs are presented and discussed in Section III.

II. ANALYSIS OF H-PLANE FILTERS BY THE CIET

The theory is presented for the example of a four-resonator filter structure which is depicted in Fig. 1. It consists of a lossless rectangular waveguide of cross section $a \times b$ and five symmetric H-plane irises of thickness d. The apertures of the irises are $a_i = a - 2b_i$ where b_i is the width of one side of the ith iris.
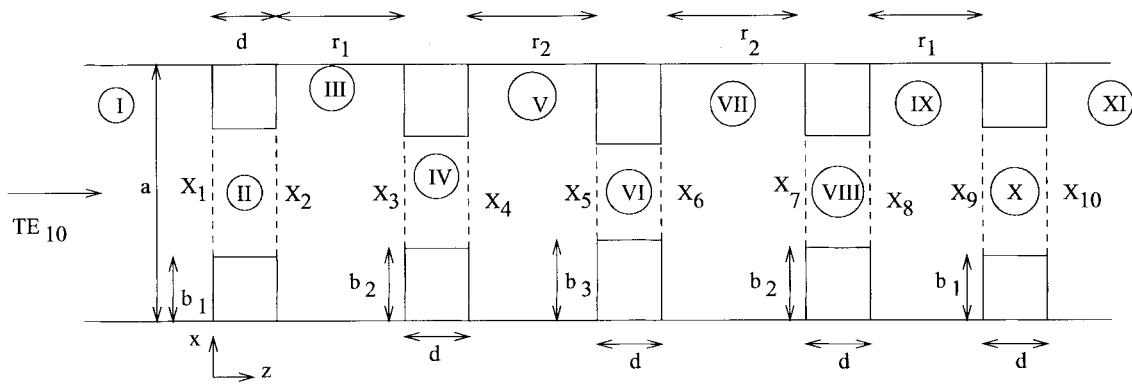
Fig. 1. Side view of a symmetric four-resonator H-plane filter.

In most applications, only the fundamental TE_{10} mode is incident, with amplitude unity on one side of the structure, which is taken as the left side in Fig. 1.

Because of the symmetry of the irises, only TE_{m0} modes, with m, an odd integer, are excited in the structure. Following the MMT, we expand the transverse electric and magnetic fields in each of the subregions I–XI in modal series.

In region I, there are reflected waves in addition to the incident fundamental mode. In all the inner sections, there are both forward- and backward-traveling waves, whereas only forward-traveling modes are present in the right-most section. Therefore, in region I we have the following expansion [1]:

$$E_y^I(x) = \sin\left[\pi\frac{x}{a}\right]e^{-jk_1^I z} + \sum_{m=1}^{\infty} B_m^I \sin\left[m\pi\frac{x}{a}\right]e^{jk_m^I z} \tag{1a}$$

and

$$H_x^I(x)$$
$$= -Y_1^I \sin\left[\pi\frac{x}{a}\right]e^{-jk_1^I z} + \sum_{m=1}^{\infty} Y_m^I B_m^I \cdot \sin\left[m\pi\frac{x}{a}\right]e^{jk_m^I z}. \tag{1b}$$

In the internal regions $i =$ III, V, VII, IX, the transverse electric and magnetic fields are a superposition of forward– and backward-traveling modes

$$E_y^i(x) = \sum_{m=1}^{\infty} (F_m^i e^{-jk_m^i z} + B_m^i e^{jk_m^i z}) \sin\left[m\pi\frac{x}{a}\right] \tag{2a}$$

and

$$H_x^i(x)$$
$$= \sum_{m=1}^{\infty} Y_m^i(-F_m^i e^{-jk_m^i z} + B_m^i e^{jk_m^i z}) \sin\left[m\pi\frac{x}{a}\right]. \tag{2b}$$

In the internal regions $i =$ II, IV, VI, VIII, X, E_y and H_x are of the form

$$E_y^i(x) = \sum_{m=1}^{\infty} (F_m^i e^{-jk_m^i z} + B_m^i e^{jk_m^i z}) \sin\left[m\pi\frac{(x-b_i)}{a_i}\right] \tag{3a}$$

and

$$H_x^i(x) = \sum_{m=1}^{\infty} Y_m^i(-F_m^i e^{-jk_m^i z} + B_m^i e^{jk_m^i z})$$
$$\cdot \sin\left[m\pi\frac{(x-b_i)}{a_i}\right]. \tag{3b}$$

Finally, we have only forward-traveling waves in region XI:

$$E_y^{XI}(x) = \sum_{m=1}^{\infty} F_m^{XI} \sin\left[m\pi\frac{x}{a}\right]e^{-jk_m^{XI} z} \tag{4a}$$

$$H_x^{XI}(x) = -\sum_{m=1}^{\infty} Y_m^I F_m^X \sin\left[m\pi\frac{x}{a}\right]e^{-jk_m^{XI} z}. \tag{4b}$$

Here

$$k_m^i = \begin{cases} +\sqrt{\omega^2\epsilon_0\mu_0 - \left(\frac{m\pi}{a_i}\right)^2}, & \text{propagating mode} \\ -j\sqrt{\left(\frac{m\pi}{a_i}\right)^2 - \omega^2\epsilon_0\mu_0}, & \text{evanescent mode} \end{cases} \tag{5}$$

and

$$Y_m^i = \frac{k_m^i}{\omega\mu_0}. \tag{6}$$

The unknown modal expansion coefficients B_m^i's and F_m^i's in these expansions are determined from the boundary conditions at the discontinuities. These consist in the vanishing of E_y over the metallic part of the discontinuity and the continuity of H_x and E_y over the aperture, i.e.,

$$E_y(x) = 0, \qquad \text{over metallic step} \tag{7a}$$
$$E_y^i(x) = E_y^{i+1}(x), \qquad \text{over aperture } i \tag{7b}$$

and

$$H_x^i(x) = H_x^{i+1}(x), \qquad \text{over aperture } i. \tag{7c}$$

When the structure is operated in the frequency range where only the fundamental mode TE_{10} is propagating, and if the input and output sections are long enough for all the evanescent modes to be attenuated, the frequency response of the structure is totally determined once B_1^I and F_1^{XI} are known. Indeed, the reflected power is determined from B_1^I, whereas F_1^{XI} totally specifies the transmitted power.

Instead of following the MMT in enforcing the boundary conditions in a modular fashion, we take an approach which emphasizes two important facts: the physics of the problem takes place at the discontinuities, and what is actually of interest are the reflected and transmitted powers at the input and output. The internal reflections, although important in determining the overall response of the structure, could be viewed as additional information which is not accessible to the measuring engineer. Therefore, we compute the reflection and transmission coefficients *directly*.

To enforce the boundary conditions of the transverse electric field at the discontinuities, we assume that these are given by unknown functions $X_i(x)$. Each of these functions is assumed to vanish on the metallic part of the ith discontinuity:

$$X_i(x) = 0, \quad \left| x - \frac{a}{2} \right| > a_i/2, \qquad i = 1, 2, \cdots, 10. \quad (8)$$

The continuity of E_y [(7b)] is then rewritten in the form

$$\begin{aligned} E_y^i(x) &= X_i(x) \\ E_y^{i+1}(x) &= X_i(x). \end{aligned} \quad (9)$$

It is straightforward to verify that (7a) and (7b) are *always* satisfied as long as (8) hold.

To determine the functions $X_i(x)$, the modal expansions of the electric field are used in (9) to project out the modal coefficients B_m^i and F_m^i. For example, in the first region we get

$$\begin{aligned} B_m^{\mathrm{I}} &= -\delta_{m1} + \frac{2}{a} \int_{a-a_2/2}^{a+a_2/2} X_1(x) \sin\left[m\pi \frac{x}{a} \right] dx \\ &= -\delta_{m1} + \tilde{X}_1^{\mathrm{I}}(m). \end{aligned} \quad (10)$$

Here, the transformed function $\tilde{X}_1^{\mathrm{I}}(m)$ is given by

$$\tilde{X}_1^{\mathrm{I}}(m) = \frac{2}{a} \int_{a-a_2/2}^{a+a_2/2} X_1(x) \sin\left[m\pi \frac{x}{a} \right] dx. \quad (11)$$

On the other hand, the coefficients B_m^{II} and F_m^{II} involve the functions X_1 and X_2 and are given by

$$B_m^{\mathrm{II}} = \frac{e^{jk_m^{\mathrm{II}} d} \tilde{X}_1^{\mathrm{II}}(m) - \tilde{X}_2^{\mathrm{II}}(m)}{2j \sin\left[k_m^{\mathrm{II}} d \right]} \quad (12\mathrm{a})$$

and

$$F_m^{\mathrm{II}} = \frac{\tilde{X}_2^{\mathrm{II}}(m) - e^{-jk_m^{\mathrm{II}} d} \tilde{X}_1^{\mathrm{II}}(m)}{2j \sin\left[k_m^{\mathrm{II}} d \right]}. \quad (12\mathrm{b})$$

The notation $\tilde{X}_1^{\mathrm{II}}(m)$, which is introduced for convenience, is defined as

$$\tilde{X}_1^{\mathrm{II}}(m) = \frac{2}{a_2} \int_{a-a_2/2}^{a+a_2/2} X_1(x) \sin\left[m\pi \frac{(x - b_2)}{a_2} \right] dx. \quad (13)$$

Similar expressions hold for the modal expansion coefficients in the remaining internal regions. Finally, the modal expansion coefficients in region XI are related to X_{10} through

$$F_m^{\mathrm{XI}} = e^{jk_m^I(4d + 2r_1 + 2r_2)} \tilde{X}_{10}^I(m). \quad (14)$$

If (10)–(14) are used in the continuity conditions of H_x at the different discontinuities, we get a set of ten CIE's in the ten unknown functions $X_i(x)$. A system of coupled singular integral equations is often referred to as an RHP [3]. Applications of the RHP to diaphragms of zero thickness with one or more windows are discussed in [6].

From the continuity of H_x at interface I–II, we get the integral equation

$$\sum_{m=1}^{\infty} Y_m^{\mathrm{II}} \frac{\tilde{X}_1^{\mathrm{II}}(m) \cos\left[k_m^{\mathrm{II}} d \right] - \tilde{X}_2^{\mathrm{II}}(m)}{j \sin\left[k_m^{\mathrm{II}} d_2 \right]} \sin\left[m\pi \frac{(x - b_2)}{a_2} \right]$$
$$+ \sum_{m=1}^{\infty} Y_m^I \tilde{X}_1^I(m) \sin\left[m\pi \frac{x}{a} \right] = 2Y_1^I \sin\left[\pi \frac{x}{a} \right] \quad (15)$$

which holds only over the gap of the leftmost iris, i.e, when $|x - a/2| \le a_2/2$.

Similarly, the continuity of H_x at the second discontinuity (the right side of the leftmost iris) leads to a second intergal equation

$$\sum_{m=1}^{\infty} Y_m^{\mathrm{II}} \frac{\tilde{X}_2^{\mathrm{II}}(m) \cos\left[k_m^{\mathrm{II}} d \right] - \tilde{X}_1^{\mathrm{II}}(m)}{\sin\left[k_m^{\mathrm{II}} d \right]} \sin\left[m\pi \frac{(x - b_2)}{a_2} \right]$$
$$+ \sum_{m=1}^{\infty} Y_m^I \frac{\tilde{X}_2^I(m) \cos\left[k_m^I r_1 \right] - \tilde{X}_3^I(m)}{\sin\left[k_m^I r_1 \right]} \sin\left[m\pi \frac{x}{a} \right] = 0 \quad (16)$$

which also holds over the same range of x as (15). The integral equations for the remaining internal irises are similar to (16) and are not given here. The matrix elements which appear in the numerical solution of these equations are, however, given in the Appendix.

The continuity of H_x at the right side of the rightmost iris leads to

$$\sum_{m=1}^{\infty} Y_m^{\mathrm{II}} \frac{\tilde{X}_9^{\mathrm{II}}(m) \cos\left[k_m^{\mathrm{II}} d \right] - \tilde{X}_{10}^{\mathrm{II}}(m)}{j \sin\left[k_m^{\mathrm{II}} d \right]} \sin\left[m\pi \frac{(x - b_2)}{a_2} \right]$$
$$- \sum_{m=1}^{\infty} Y_m^I \tilde{X}_{10}^I(m) \sin\left[m\pi \frac{x}{a} \right] = 0. \quad (17)$$

Note that the symmetry of the filter was used in this equation (regions II and X are identical).

To solve this set of CIE's, we expand the functions $X_i(x)$ in a series of basis functions and apply Galerkin's method to each one of them. Let $B_{ij}(x)$ denote the jth element of a set of basis functions for the function $X_i(x)$ such that

$$X_i(x) = \sum_{j=1}^{M} c_{ij} B_{ij}(x), \qquad i = 1, \cdots, 10. \quad (18)$$

Since the nonanalytic behavior of E_y is the same at both sides of a given iris, the same basis functions are used to expand the fields at any two identical discontinuities.

If these expansion are used in the integral equations and Galerkin's method is applied to each one of a them, a set of coupled linear equations in the expansion coefficients c_{ij}'s results. The ten linear equations can be put in the following form:

$$[A^1][c_1] + [A^2][c_2] = [U] \tag{19a}$$
$$[A^3][c_1] + [A^4][c_2] + [A^5][c_3] = 0 \tag{19b}$$
$$[A^6][c_2] + [A^7][c_3] + [A^8][c_4] = 0 \tag{19c}$$
$$[A^9][c_3] + [A^{10}][c_4] + [A^{11}][c_5] = 0 \tag{19d}$$
$$[A^{12}][c_4] + [A^{13}][c_5] + [A^{14}][c_6] = 0 \tag{19e}$$
$$[A^{15}][c_5] + [A^{16}][c_6] + [A^{17}][c_7] = 0 \tag{19f}$$
$$[A^{19}][c_6] + [A^{20}][c_7] + [A^{21}][c_8] = 0 \tag{19g}$$
$$[A^{22}][c_7] + [A^{23}][c_8] + [A^{24}][c_9] = 0 \tag{19h}$$
$$[A^{25}][c_8] + [A^{26}][c_9] + [A^{27}][c_{10}] = 0 \tag{19i}$$

and

$$[A^{28}][c_9] + [A^{29}][c_{10}] = 0. \tag{19j}$$

The entries of the matrices in (19a)–(19j) are given in the Appendix. It is worth noting that most of these matrices are symmetrical, a fact which is used to reduce the computational effort. In addition, for the symmetric filter under investigation, only 14 of the 29 matrices are independent; a considerable reduction in central-processing-unit (CPU) time results. Also note that (19b)–(19i) follow a clear pattern which allows the number of resonators and irises to be varied relatively simple.

To complete the numerical solution, appropriate sets of basis function are needed.

III. BASIS FUNCTIONS

To guarantee numerical efficiency, the basis functions should include the nonanalytic behavior of E_y at the edges of the irises. At a 90° metallic wedge, E_y vanishes as $r^{2/3}$ as the radial distance to the axis of the wedge r approaches zero [7]. Note also that E_y is also an even function with respect to the axis of the filter as only TE_{m0} modes with m odd are excited. A set of basis functions which satisfy these conditions are given by

$$B_{ik}(x) = \frac{\sin\left[k\pi\dfrac{(x - b_i)}{a_i}\right]}{[(x - b_i)(a_i + b_i - x)]^{1/3}}, \quad k = 1, 2, \cdots. \tag{20}$$

Because of the symmetry of the filter with respect to the central iris, only three different sets of basis functions are needed.

The spectra of these basis functions, the integrals appearing in the integral equations and the matrices (19) (see Appendix), are expressible in terms of Bessel functions of the first kind

of order $1/6$ $(G = 0.5\Gamma(1/2)\Gamma(2/3))$ [8]:

$$\tilde{B}_{1k}^{II}(m) = G\left\{\frac{J_{1/6}\left[\left|\dfrac{m-k}{2}\pi\right|\right]}{\left|\dfrac{m-k}{4}\pi\right|^{1/6}}\cos\left[\dfrac{m-k}{2}\pi\right]\right.$$
$$\left. - \frac{J_{1/6}\left[\dfrac{m+k}{2}\pi\right]}{\left|\dfrac{m+k}{4}\pi\right|^{1/6}}\cos\left[\dfrac{m+k}{2}\pi\right]\right\} \tag{21a}$$

$$\tilde{B}_{5k}^{VI}(m) = \tilde{B}_{3k}^{IV}(m) = \tilde{B}_{1k}^{II}(m) \tag{21b}$$

$$\tilde{B}_{1k}^{I}(m) = G\frac{a_2}{a}\left\{\frac{J_{1/6}\left[\left|\dfrac{\pi}{2}\left(m\dfrac{a_2}{a} - k\right)\right|\right]}{\left|\dfrac{\pi}{4}\left(m\dfrac{a_2}{a} - k\right)\right|^{1/6}}\cos\left[\dfrac{\pi}{2}(m - k)\right]\right.$$
$$\left. - \frac{J_{1/6}\left[\dfrac{\pi}{2}\left(m\dfrac{a_2}{a} + k\right)\right]}{\left|\dfrac{\pi}{4}\left(m\dfrac{a_2}{a} + k\right)\right|^{1/6}}\cos\left[\dfrac{\pi}{2}(m + k)\right]\right\}. \tag{21c}$$

The quantities $\tilde{B}_{3k}^{I}(m)$ and $\tilde{B}_{5k}^{I}(m)$ are obtained from $\tilde{B}_{1k}^{I}(m)$ by replacing a_2 by a_4 and a_6, respectively.

Despite the fact that these spectra involve a Bessel function of order $1/6$, most of the terms in the sums in the entries of matrices (19) involve large arguments where the asymptotic forms of Bessel functions can be used without sacrificing accuracy. A routine for computing Bessel functions of fractional order can be found in [9].

IV. NUMERICAL RESULTS

The CIET and the MMT are applied to the analysis of two four-resonator H-plane filters to compare their performances with regards to CPU time and accuracy.

All irises are 1-mm thick in the first filter with heights $b_1 = 4.339$, $b_2 = 6.086$, and $b_3 = 6.43$ mm, and separations $r_1 = 15.712$ and $r_2 = 17.671$ mm. The main rectangular waveguide is a WR75.

The numerical results for the return loss of the first filter as obtained from the two techniques are shown in Fig. 2(a). In the MMT (dashed line), 18 odd modes are used in the larger waveguide sections. The number of modes in the irises are taken according to the respective aperture-width ratios [2]. In the CIET solution (solid line), only one basis function was used. A reduction of CPU time of the order of 200 over the MMT is observed. More basis functions were also used and led to only minor changes, which are shown in Fig. 2(b) for $M = 1, 2, 3$, and four basis functions. The rapid convergence of the solution reflects the judicious choice of the basis functions as well as the fact that the internal reflections are all taken into account by testing the sums in (19a)–(19j) for convergence. Good agreement between the two techniques is observed. Note that the sums in the entries of the matrices in (19a)–(19j) involve terms which decrease at least as $n^{-7/3}$ for large n—30 terms were sufficient to reach convergence. In
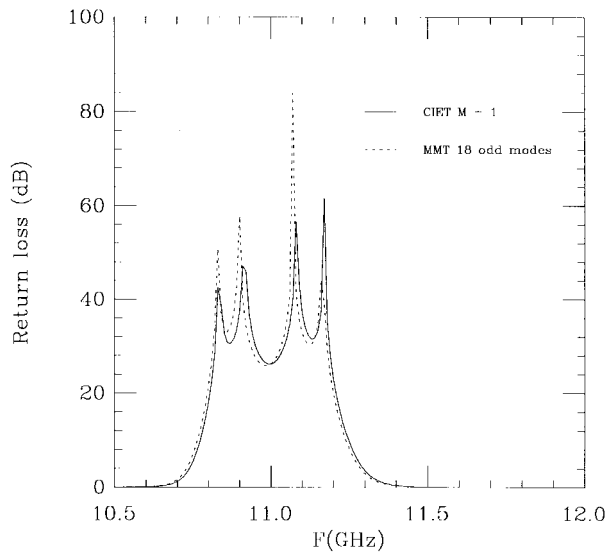
(a)
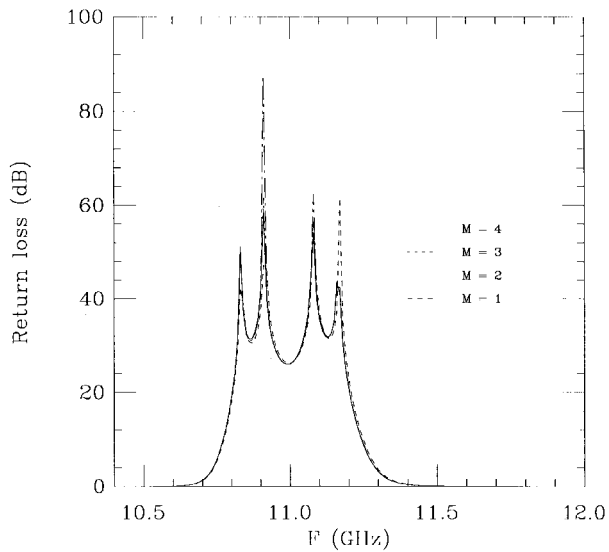
(b)

Fig. 2. Return loss (dB) of filter I as a function of frequency (a) as obtained from the CIET (solid line) with one basis function and the MMT (dashed line) with 18 odd modes and (b) when $M = 1, 2, 3$, and four basis functions are used in the CIET.
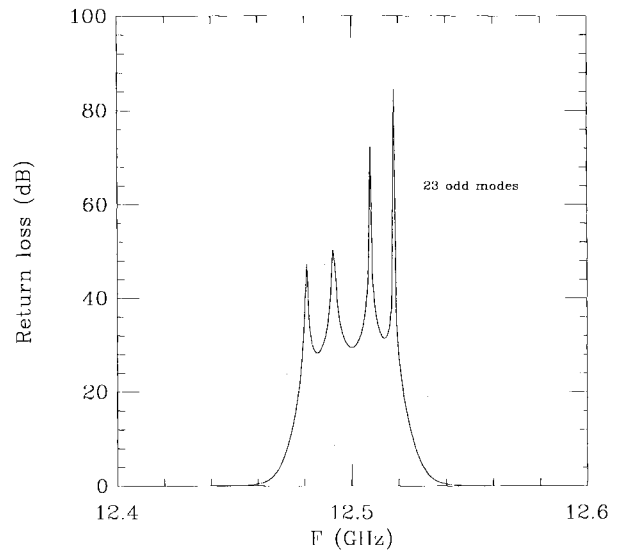

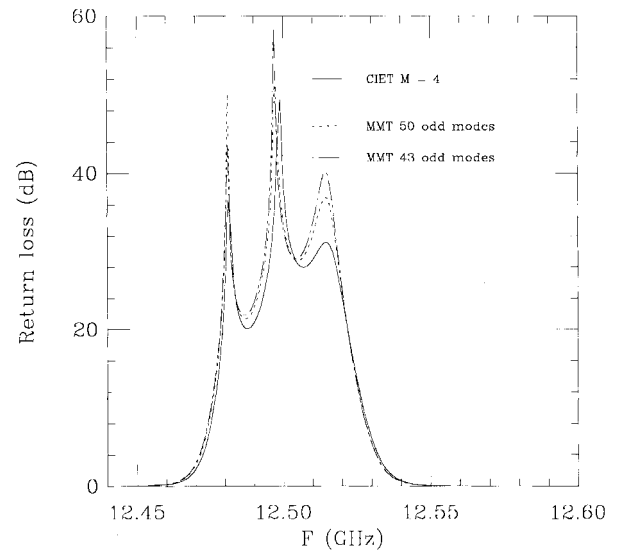Fig. 3. Return loss (dB) of filter II as obtained from the MMT with 23 odd modes.

Fig. 4. Return loss (dB) of filter II as obtained from the CIET (solid line) with four basis functions and the MMT with 43 and 50 odd modes. The CIET reduces CPU time by a factor of 400.

addition, these sums can be accelerated using the asymptotic forms of the kernels of the integral equations, the remaining terms in the sums decrease as $n^{-7/3}$ for large n.

The second filter, a 40-MHz 28-dB return-loss level filter, was designed using standard filter synthesis in combination with the MMT [1], [10]. Assuming a Q-efficiency of approximately 70% and a silver-plated filter structure, insertion losses of 1.9 dB are predicted. Although applications of such a narrow-band filter are limited (e.g., remotely operated ground-satellite and ground-to-ground links—this example was chosen specifically to highlight the characteristics of the two methods).

All irises are 1-mm thick in the second filter with heights $b_1 = 6.468$, $b_2 = 8.156$, and $b_3 = 8.285$ mm, and separations $r_1 = 14.49$ and $r_2 = 15.188$ mm. The main waveguide is a WR75.

Fig. 3 shows the return loss of such a filter as obtained from the MMT when 23 odd modes are used in the design (synthesis) and analysis process.

At first it was surprising to see the numerical results obtained from the CIET deviate markedly from what is shown in Fig. 3. We, therefore, conducted a convergence study for this filter for both methods.

Fig. 4 shows the return loss of this filter as obtained from the CIET (solid line) with four edge-conditioned basis functions and the MMT. As the number of modes in the MMT increases, the numerical results of the MMT approach those obtained from the CIET. However, even with 50 odd modes, the MMT has not reached convergence yet. This is demonstrated in Fig. 4 where the two right-most poles of Fig. 3 are shown to merge. The CPU-time comparison between the MMT with 50 odd modes and the CIET with four edge-conditioned basis
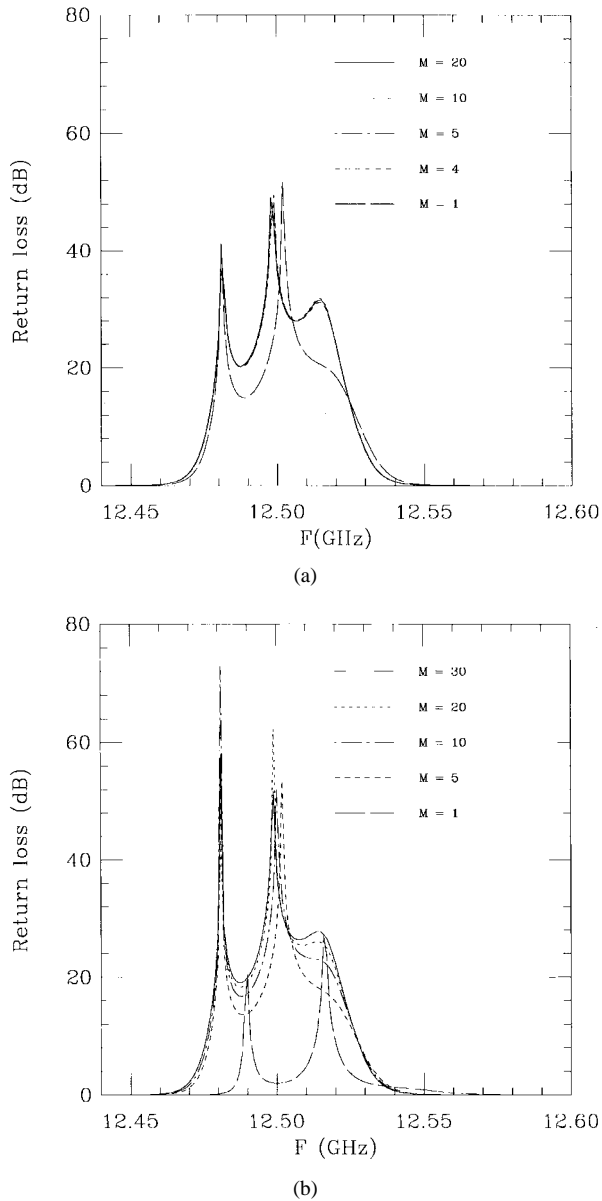
Fig. 5. Return loss of filter II when (a) basis functions with the edge conditions are used and (b) the modes of the irises are used as basis functions. The effect of the edge conditions on the convergence of the solution is evident.

functions amounts to a factor of 400. The MMT takes 9106 s on an IBM 6000 RS/530, whereas the CIET takes only 22 s for the same number of frequency points (201) and on the same machine.

The convergence of the CIET is shown in Fig. 5(a) for $M = 1, 4, 5, 10,$ and 20 basis functions. Convergence is reached with only four basis functions.

The effect of including the edge conditions on the numerical solution within the CIET was investigated. Fig. 5(b) shows the return loss of the second filter when the modes of the irises are used as basis functions. Obviously, the effect of the edge conditions is dramatic as one needs 30 basis functions or more to reproduce the results obtained with only four basis functions, which include the edge conditions. In all the calculations relating to filter II, 100 terms were summed in computing the entries of the matrices (19a)–(19j).

Finally, a few remarks about the case of zero-thickness irises. Within such an approximation, the number of integral equations to be solved is reduced by a factor of two, which results in a reduction of CPU time over the nonzero thickness. In addition, the edge condition, which is well represented by a Maxwellian, is straightforwardly included in the basis functions [5], [11].

It is also obvious that the CPU time of the CIET increases with the number of discontinuities N_s. However, it is not obvious that it increases linearly with N_s. To prove this point, we make use of the important fact that the matrix giving the expansion coefficients [equivalent of (19a)–(19j)] is *block tridiagonal*. Let us assume that N_b basis functions are used at each of the N_s discontinuities. Let c_k be the number of nonzero entries below the diagonal in column k, and r_k the number of nonzero entries to the right of the main diagonal in row k. Then the total cost of Gaussian elimination is given by the expression [12, p. 57]

$$T = 2 \sum_{k=1}^{N_s N_b - 1} c_k r_k + \sum_{k=1}^{N_s N_b - 1} c_k. \qquad (22)$$

Since the same number of basis functions are used at each discontinuity, all $c_k = r_k = 2N_b - 1$ except for $N_s N_b \leq k \leq N_s N_b$ where $0 \leq r_k \leq 2N_b - 1$. The total cost in (22) is then

$$T \leq 2(N_s N_b - 1)(2N_b - 1)^2 + (N_s N_b - 1)(2N_b - 1)$$
$$= (N_s N_b - 1)(2N_b - 1)(4N_b - 1). \qquad (23)$$

Furthermore, back substitution adds a cost of $2(N_s N_b - 1)(2N_b - 1)$ such that the total cost is proportional to $N_s N_b^3$ for large values of N_s and N_b, i.e.,

$$\text{Total cost} \propto N_s N_b^3. \qquad (24)$$

Since the number of basis functions with the edge conditions is much smaller than the number of modes in the MMT, the CIET is expected to outperform the MMT for an arbitrary number of discontinuities. It is also worth noting that the CPU time comparisons we carried out for the two filters described here were done without taking advantage of the sparsity of the matrix in the CIET.

V. CONCLUSIONS

The CIET was applied to the analysis of H-plane waveguide filters. The frequency response of the filter is determined from a set of CIE's in a *single step*. Numerical results show excellent agreement with those obtained from the MMT with a reduction of CPU time by a factor of the order of 400, especially for narrow-band filters. A few basis functions with the edge conditions at each discontinuity are sufficient to guarantee accuracy of numerical results. The inclusion of the edge conditions in the theory is essential in reducing CPU time and increasing accuracy. The technique can be straightforwardly applied to E-plane filters and double-plane waveguide filters.

APPENDIX

In this appendix we give the expressions of the entries of matrices (19a)–(19j):

$$[A^1]_{kl} = \sum_{m=1}^{\infty} Y_m^{\mathrm{I}} \tilde{B}_{1k}^{\mathrm{I}}(m) \tilde{B}_{1l}^{\mathrm{I}}(m) - j\frac{a_2}{a} \sum_{m=1}^{\infty} \cot[k_m^{\mathrm{II}} d]$$
$$\cdot Y_m^{\mathrm{II}} \tilde{B}_{1k}^{\mathrm{II}}(m) \tilde{B}_{1l}^{\mathrm{II}}(m) \tag{A1}$$

$$[A^2]_{kl} = j\frac{a_2}{a} \sum_{m=1}^{\infty} Y_m^{\mathrm{II}} \frac{\tilde{B}_{1k}^{\mathrm{II}}(m) \tilde{B}_{1l}^{\mathrm{II}}(m)}{\sin[k_m^{\mathrm{II}} d]} \tag{A2}$$

$$[U]_k = 2Y_1^{\mathrm{I}} \tilde{B}_{1k}^{\mathrm{I}}(1) \tag{A3}$$

$$[A^3]_{kl} = j[A^2]_{kl} \tag{A4}$$

$$[A^4]_{kl} = \sum_{m=1}^{\infty} Y_m^{\mathrm{I}} \cot[k_m^{\mathrm{I}} r_1] \tilde{B}_{1k}^{\mathrm{I}}(m) \tilde{B}_{1l}^{\mathrm{I}}(m)$$
$$+ \frac{a_2}{a} \sum_{m=1}^{\infty} Y_m^{\mathrm{II}} \cot[k_m^{\mathrm{II}} d] \tilde{B}_{1k}^{\mathrm{II}}(m) \tilde{B}_{1l}^{\mathrm{II}}(m) \tag{A5}$$

$$[A^5]_{kl} = -\sum_{m=1}^{\infty} Y_m^{\mathrm{I}} \frac{\tilde{B}_{1k}(m) \tilde{B}_{1l}^{\mathrm{I}}(m)}{\sin[k_m^{\mathrm{I}} r_1]} \tag{A6}$$

$$[A^6]_{kl} = -\sum_{m=1}^{\infty} Y_m^{\mathrm{I}} \frac{\tilde{B}_{3k}^{\mathrm{I}}(m) \tilde{B}_{1l}^{\mathrm{I}}(m)}{\sin[k_m^{\mathrm{I}} r_1]} \tag{A7}$$

$$[A^7]_{kl} = \sum_{m=1}^{\infty} Y_m^{\mathrm{I}} \cot[k_m^{\mathrm{I}} r_1] \tilde{B}_{3k}^{\mathrm{I}}(m) \tilde{B}_{3l}^{\mathrm{I}}(m)$$
$$+ \frac{a_4}{a} \sum_{m=1}^{\infty} Y_m^{\mathrm{IV}} \cot[k_m^{\mathrm{IV}} d] \tilde{B}_{1k}^{\mathrm{II}}(m) \tilde{B}_{1l}^{\mathrm{II}}(m) \tag{A8}$$

$$[A^8]_{kl} = -\frac{a_4}{a} \sum_{m=1}^{\infty} Y_m^{\mathrm{IV}} \frac{\tilde{B}_{1k}^{\mathrm{II}}(m) \tilde{B}_{1l}^{\mathrm{II}}(m)}{\sin[k_m^{\mathrm{IV}} d]} \tag{A9}$$

$$[A^9]_{kl} = [A^8]_{kl} \tag{A10}$$

$$[A^{10}]_{kl} = \sum_{m=1}^{\infty} Y_m^{\mathrm{I}} \cot[k_m^{\mathrm{I}} r_2] \tilde{B}_{3k}^{\mathrm{I}}(m) \tilde{B}_{3l}^{\mathrm{I}}(m)$$
$$+ \frac{a_4}{a} \sum_{m=1}^{\infty} Y_m^{\mathrm{IV}} \cot[k_m^{\mathrm{IV}} d] \tilde{B}_{1k}^{\mathrm{II}}(m) \tilde{B}_{1l}^{\mathrm{II}}(m) \tag{A11}$$

$$[A^{11}]_{kl} = -\sum_{m=1}^{\infty} Y_m^{\mathrm{I}} \frac{\tilde{B}_{3k}^{\mathrm{I}}(m) \tilde{B}_{5l}^{\mathrm{I}}(m)}{\sin[k_m^{\mathrm{I}} r_2]} \tag{A12}$$

$$[A^{12}]_{kl} = [A^{11}]_{lk} \tag{A13}$$

$$[A^{13}]_{kl} = \sum_{m=1}^{\infty} Y_m^{\mathrm{I}} \cot[k_m^{\mathrm{I}} r_2] \tilde{B}_{5k}^{\mathrm{I}}(m) \tilde{B}_{5l}^{\mathrm{I}}(m)$$
$$+ \frac{a_6}{a} \sum_{m=1}^{\infty} Y_m^{\mathrm{VI}} \cot[k_m^{\mathrm{VI}} d] \tilde{B}_{1k}^{\mathrm{II}}(m) \tilde{B}_{1l}^{\mathrm{II}}(m) \tag{A14}$$

$$[A^{14}]_{kl} = -\frac{a_6}{a} \sum_{m=1}^{\infty} Y_m^{\mathrm{VI}} \frac{\tilde{B}_{1k}^{\mathrm{II}}(m) \tilde{B}_{1l}^{\mathrm{II}}(m)}{\sin[k_m^{\mathrm{VI}} d]} \tag{A15}$$

$$[A^{15}]_{kl} = [A^{14}]_{kl} \tag{A16}$$

$$[A^{16}]_{kl} = \sum_{m=1}^{\infty} Y_m^{\mathrm{I}} \cot[k_m^{\mathrm{I}} r_2] \tilde{B}_{5k}^{\mathrm{I}}(m) \tilde{B}_{5l}^{\mathrm{I}}(m)$$
$$+ \frac{a_6}{a} \sum_{m=1}^{\infty} Y_m^{\mathrm{VI}} \cot[k_m^{\mathrm{VI}} d] \tilde{B}_{1k}^{\mathrm{II}}(m) \tilde{B}_{1l}^{\mathrm{II}}(m) \tag{A17}$$

$$[A^{17}]_{kl} = [A^{12}]_{kl} \tag{A18}$$

$$[A^{18}]_{kl} = [A^{12}]_{kl} \tag{A19}$$

$$[A^{19}]_{kl} = [A^{10}]_{kl} \tag{A20}$$

$$[A^{20}]_{kl} = [A^9]_{kl} \tag{A21}$$

$$[A^{21}]_{kl} = [A^9]_{kl} \tag{A22}$$

$$[A^{22}]_{kl} = [A^7]_{kl} \tag{A23}$$

$$[A^{23}]_{kl} = [A^6]_{kl} \tag{A24}$$

$$[A^{24}]_{kl} = [A^6]_{kl} \tag{A25}$$

$$[A^{25}]_{kl} = [A^4]_{kl} \tag{A26}$$

$$[A^{26}]_{kl} = [A^3]_{kl} \tag{A27}$$

$$[A^{27}]_{kl} = -j\frac{a_2}{a} \sum_{m=1}^{\infty} Y_m^{\mathrm{II}} \frac{\tilde{B}_{1k}^{\mathrm{II}}(m) \tilde{B}_{1l}^{\mathrm{II}}(m)}{\sin[k_m^{\mathrm{II}} d]} \tag{A28}$$

$$[A^{28}]_{kl} = -\sum_{m=1}^{\infty} Y_m^{\mathrm{I}} \tilde{B}_{1k}^{\mathrm{I}}(m) \tilde{B}_{1l}^{\mathrm{I}}(m)$$
$$+ j\frac{a_2}{a} \sum_{m=1}^{\infty} Y_m^{\mathrm{II}} \cot[k_m^{\mathrm{II}} d] \tilde{B}_{1k}^{\mathrm{I}}(m) \tilde{B}_{1l}^{\mathrm{I}}(m). \tag{A29}$$

REFERENCES

[1] J. Uher, J. Bornemann, and U. Rosenberg, *Waveguide Components for Antenna Feed Systems: Theory and CAD*. Norwood, MA: Artech House, 1993.

[2] T. Itoh, Ed., *Numerical Techniques for Microwave and Millimeter-Wave Passive Structures*. New York: Wiley, 1989.

[3] N. P. Vekua, *Systems of Singular Integral Equations*. Noordhoff, The Netherlands: Groningen, 1967.

[4] S. Amari, J. Bornemann, and R. Vahldieck, "Accurate analysis of scattering from multiple waveguide discontinuities using the coupled-integral-equations technique," *J. Electromagnetic Waves Appl.*, vol. 10, pp. 1623–1644, 1996.

[5] ——, "Application of a coupled-integral-equations technique to ridged waveguides," *IEEE Trans. Microwave Theory Tech.*, vol. 44, pp. 2256–2264, Dec. 1996.

[6] L. Lewin, *Theory of Waveguides*. London, U.K.: Newnes–Butterworths, 1975.

[7] R. E. Collin, *Field Theory of Guided Waves*. Piscataway, NJ: IEEE Press, 1991.

[8] I. S. Gradshteyn and I. M. Ryznik, *Tables of Integrals, Series, and Products*, 5th ed. New York: Academic, 1994.

[9] W. H. Press, B. P. Flannery, S. A. Teukolsky, and W. T. Vetterling, *Numerical Recipes—The Art of Scientific Computing*, 2nd ed. Cambridge, U.K.: Cambridge Univ. Press, 1994.

[10] G. Mattthaei, L. Young, and E. M. T. Jones, *Microwave Filters Impedance-Matching Networks, and Coupling Structures*. Norwood, MA: Artech House, 1985.

[11] S. Amari, J. Bornemann, and R. Vahldieck, "A comparative study of two integral formulations for inductive irises in rectangular waveguides," *Proc. Inst. Elect. Eng.—Microwave Antennas Propagat.*, vol. 143, pp. 483–486, Dec. 1996.

[12] I. S. Duff, A. M. Erisman, and J. K. Reid, *Direct Methods for Sparse Matrices*. Oxford, U.K.: Clarendon Press, 1986.

Smain Amari received the D.E.S. degree in physics and electronics from Constantine University, Algeria, in 1985, and the M.S. degree in electrical engineering and the Ph.D. degree in physics, from Washington University, St. Louis, MO, in 1989 and 1994, respectively.

Since 1994, he has been with the Department of Electrical and Computer Engineering at the University of Victoria, Victoria, B.C., Canada. His research interests are in numerical methods in electromagnetics, numerical analysis, applied mathematics, applied physics and application of quantum field theory in quantum many-particle systems.

Jens Bornemann (M'87–SM'90) was born in Hamburg, Germany, on May 26, 1952. He received the Dipl.-Ing. and the Dr.-Ing. degrees, both in electrical engineering, from the University of Bremen, Bremen, Germany, in 1980 and 1984, respectively.

From 1980 to 1983, he was a Research and Teaching Assistant in the Microwave Department, University of Bremen, where he worked on quasi-planar waveguide configurations and computer-aided E-plane filter design. In 1985, after a two-year period as a Consulting Engineer, he joined the University of Bremen again as an Assistant Professor. Since April 1988, he has been with the University of Victoria, Victoria, B.C., Canada, where he is currently a Professor in the Department of Electrical and Computer Engineering. His research activities include microwave/millimeter-wave components and systems design, and problems of electromagnetic field theory in integrated circuits and radiating structures. He is a coauthor of *Waveguide Components for Antenna Feed Systems. Theory and Design* (Artech House, 1993) and has authored/co-authored over 110 technical papers.

Dr. Bornemann is a Registered Professional Engineer in the Province of British Columbia, Canada. He serves on the editorial boards of the IEEE TRANSACTIONS ON MICROWAVE THEORY AND TECHNIQUES and the *International Journal Of Numerical Modeling*. From 1992 to 1995, he was a Fellow of the British Columbia Advanced Systems Institute, and was one of the recipients of the A. F. Bulgin Premium of the Institution of Electronic and Radio Engineers in 1983.

Rüdiger Vahldieck (M'85–SM'86) received the Dipl.-Ing. and the Dr.-Ing. degrees in electrical engineering from the University of Bremen, Bremen, Germany, in 1980 and 1983, respectively.

From 1984 to 1986, he was a Research Associate at the University of Ottawa, Ottawa, Ont., Canada. In 1986, he joined the University of Victoria, Victoria, B.C., Canada, where he became a Full-Professor in the Department of Electrical and Computer Engineering in 1991. During the Fall and Spring of 1992–1993, he was a Visiting Scientist at the Ferdinand-Braun-Institute für Hochfrequenztechnik, Berlin, Germany. Since October 1996, he has been the Chair for Field Theory at the Laboratory for Electromagnetic Fields and Microwave Electronics at the Swiss Federal Institute of Technology in Zurich, Switzerland. He has published over 150 technical papers. His research interest include numerical methods to model electromagnetic fields for computer-aided design of microwave, millimeter-wave, and opto-electronic integrated circuits. He is also interested in the design and simulation of devices and subsystems for broad-band fiber-optic communication systems.

Dr. Vahldieck, together with three co-authors, received the outstanding publication award of the Institution of Electronic and Radio Engineers in 1983. He is on the editorial board of the IEEE TRANSACTION ON MICROWAVE THEORY AND TECHNIQUES, and since 1992, has served on the technical program committee of the IEEE International Microwave Symposium.